Diagnosing Low-Mode ($\ell < 6$) and Mid-Mode ($6 \leq \ell \leq 60$) Asymmetries in the Post-Stagnation Phase of Cryogenic Implosions on OMEGA

J. Baltazar,[1,2] R. Betti,[1,2] K. Churnetski,[1,2] V. Gopalaswamy,[1] J. P. Knauer,[1] D. Patel,[1] H. G. Rinderknecht,[1] R. C. Shah,[1] C. Stoeckl,[1] C. A. Williams,[1] and S. P. Regan[1,2]

[1]Laboratory for Laser Energetics, University of Rochester
[2]Department of Mechanical Engineering, University of Rochester

In order to achieve ignition-relevant conditions in direct-drive inertial confinement fusion (ICF) implosions, the hot spot must reach pressures exceeding ~100 Gbar (Ref. 1). Simulations of 1-D implosions predict that these pressures can be achieved by driving low- ($\alpha < 3$) to mid-adiabat ($\alpha > 4$) implosions, where mid-adiabat implosions require mitigation of cross-beam energy transfer (CBET) losses.[2] The performance of low-adiabat implosions is sensitive to ablation-surface modulations caused by target features and laser nonuniformity imprint, which becomes the seed for the Rayleigh–Taylor instability.[3] On some high-performance implosions[4] with $\alpha > 4$, CBET losses are mitigated by reducing the laser beam size, which reduces the ratio of the beam radius (R_b) to the initial target radius (R_t) below one and increases the laser coupling. Simulations predict that by increasing the on-target laser coupling, the hydrodynamic efficiency increases. However, this change also increases beam-overlap perturbations that causes distortions in the dense shell and leads to shell breakup at stagnation.[2] An interesting approach to diagnose the shell breakup was inspired by previous work at Lawrence Livermore National Laboratory,[5] where low modes were diagnosed by self-emission imaging in the explosion phase of DT cryogenic indirectly driven ICF implosions that were not diagnosed in the stagnation phase.

In this study, x-ray self-emission from the implosions is recorded with a filtered 16-pinhole array imager and an x-ray framing camera (XRFC) to produce gated-images of x-ray emission.[3,6] A 0.3-μm aluminum and 1-μm polypropylene filter is employed to record x rays with energies >800 eV. The framing camera is timed to record images in the explosion phase. A 3-D *ASTER*[2] simulation of a DT cryogenic implosion has been post-processed through *Spect3D*[7] to produce synthetic x-ray images that are analyzed to investigate x-ray signatures of the shell breakup. The synthetic images are integrated over 40 ps and blurred with 20-μm FWHM to match the instrument response function of the XRFC. The 3-D *ASTER* simulation was run with phase plates to produce a smaller beam radius compared to the radius of the target ($R_b/R_t \sim 0.75$) The evolution of the density, temperature, and emission from the deceleration phase to the post-stagnation (explosion) phase is shown in Fig. 1. The reduced R_b/R_t leads to an increase in beam-mode perturbations that evolve throughout the deceleration, stagnation, and explosion phase, where in the explosion phase the perturbed features are more apparent compared to the previous stages.

Figure 2 shows experimental images obtained in implosion using setups with different R_b/R_t. A Fourier decomposition is applied to the outer peak signal of the images to diagnose the low- and mid-mode asymmetries in the implosion. The images are first mapped onto a radius and angle coordinate system, where the radius is the distance from the center and the angle corresponds with the angle with respect to the x axis. The modal analysis for two implosions with different R_b/R_t is shown in Fig. 2(c). The implosion with $R_b/R_t \sim 0.77$ shows higher low- and mid-mode amplitudes compared with the implosion with $R_b/R_t \sim 0.95$. At a larger R_b/R_t, more beams overlap at the target surface, which leads to a more-uniform laser-intensity profile, less hydro instability seeds in the low/mid spatial modes, and lower measured mode amplitudes.

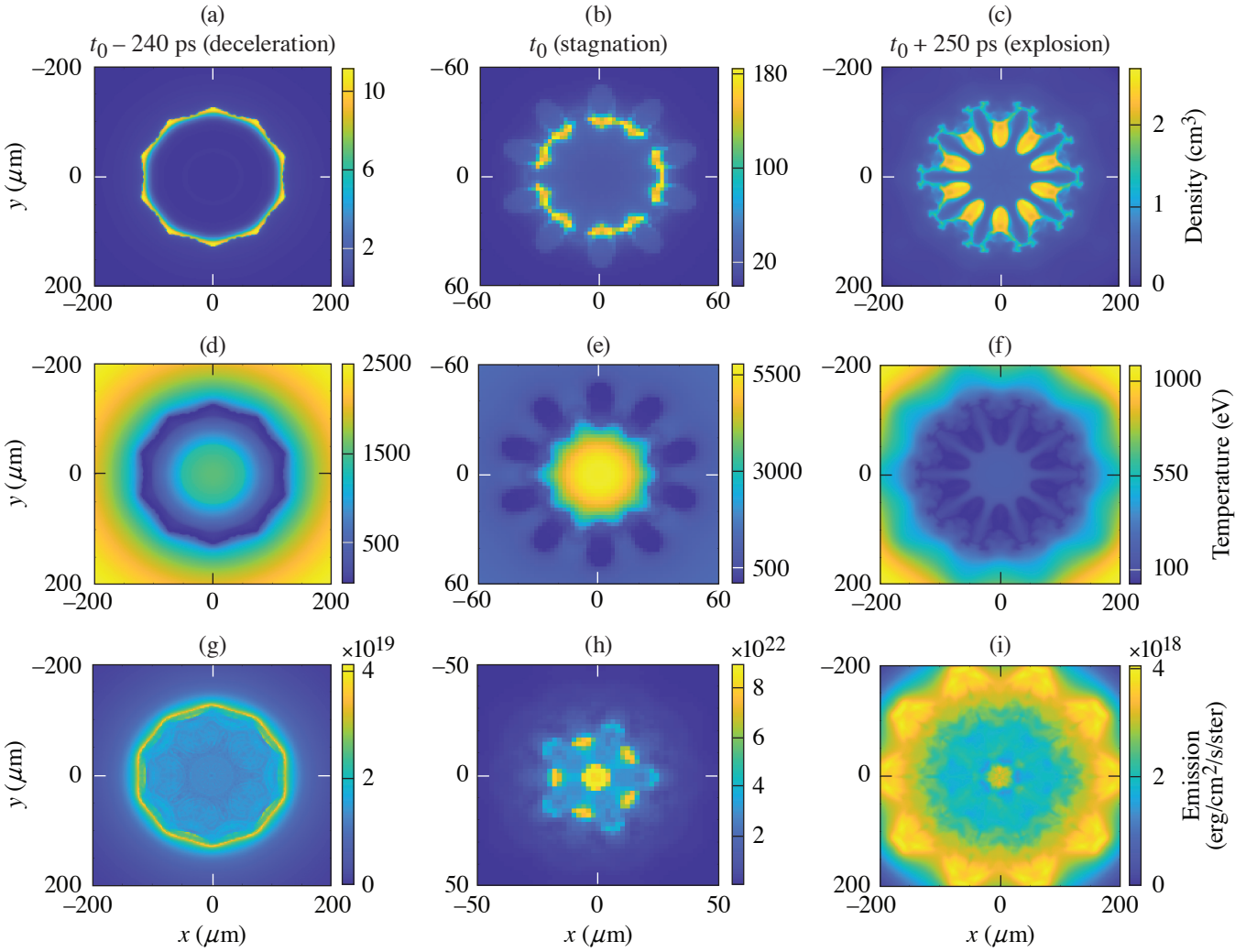

Figure 1
Evolution of the [(a)–(c)] density, [(d)–(f)] temperature, and [(g)–(i)] x-ray emission during the deceleration, stagnation, and explosion phases of a cryogenic DT implosion with a $R_b/R_t \sim 0.75$ (3-D *ASTER* simulation). The low-density regions in the shell in the deceleration phase correspond to the regions of the shell that are broken during the stagnation and post-stagnation phases. Therefore, the shell nonuniformity is seeded by the beam perturbation and leads to the breakup of the shell. The post-stagnation phase x-ray image resembles the density profile and the brightest regions in the image correspond to the broken shell locations where material is being ejected. Compared to the deceleration and stagnation phase, the signature in the post-stagnation phase x-ray measurement is spatially larger and is easier to analyze.

In conclusion, a technique was developed to diagnose the low- and mid-mode asymmetries in the explosion phase of a DT cryogenic implosion. This technique is developed with the aim of relating the explosion phase measurement to the shell breakup caused by an increase in beam overlap perturbations due to a lower R_b/R_t. An R_b/R_t sensitivity analysis from explosion phase measurements on OMEGA shows that the mid-mode rms value increases as the R_b/R_t value decreases, which is expected due to an increase in nonuniformity from the reduced beam overlap. A Monte Carlo simulation is underway to determine the error in the measurements and to guide the necessary changes in experimental setup to obtain better measurements.

This material is based upon work supported by the Department of Energy National Nuclear Security Administration under Award Number DE-NA0003856, the University of Rochester, and the New York State Energy Research and Development Authority.

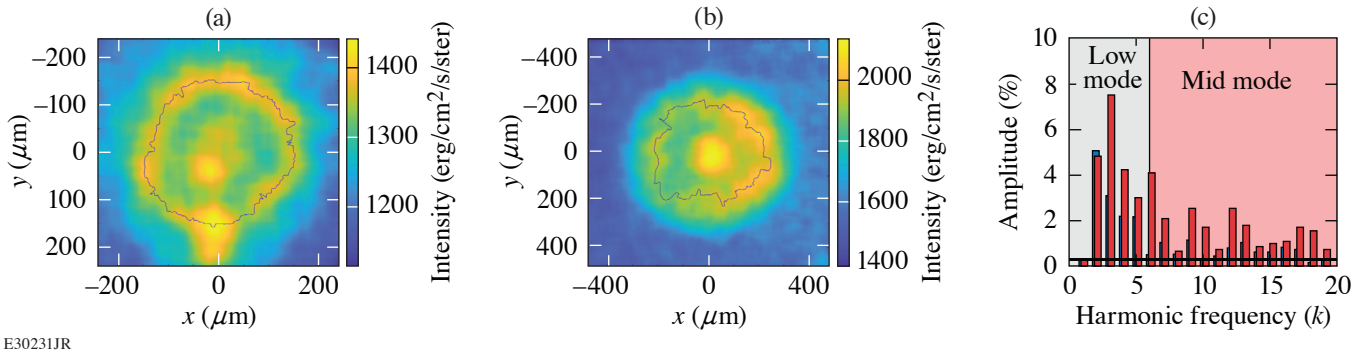

Figure 2
Experimental measurements for implosions with an R_b/R_t of (a) 0.95 and (b) 0.77. (c) The mode spectrum is plotted for both implosions [red is the analysis for the image shown in (a) and blue is the analysis for the image shown in (b)] and shows higher low- and mid-modes for the implosion with a lower R_b/R_t.

1. V. N. Goncharov *et al.*, Phys. Plasmas **21**, 056315 (2014).
2. I. V. Igumenshchev *et al.*, Phys. Plasmas **23**, 052702 (2016).
3. S. X. Hu *et al.*, Phys. Plasmas **23**, 102701 (2016).
4. V. Gopalaswamy *et al.*, Nature **565**, 581 (2019); A. Lees *et al.*, Phys. Rev. Lett. **127**, 105001 (2021).
5. A. Pak *et al.*, Phys. Plasmas **20**, 056315 (2013).
6. D. T. Michel *et al.*, Rev. Sci. Instrum. **83**, 10E530 (2012).
7. Prism Computational Sciences, Inc., Madison, WI 53711.